The Effect of Teflon™ Coatings in Polyethylene Capillary Extrusion

SAVVAS G. HATZIKIRIAKOS,[1,*] PETER HONG,[1] WALLY HO,[1] and CHARLES W. STEWART[2]

[1]Department of Chemical Engineering, The University of British Columbia, Vancouver, B.C., V6T 1Z4, Canada;
[2]DuPont Fluoroproducts, DuPont & De Nemours Co., P.O. Box 80713, Wilmington, Delaware 19880-0713

SYNOPSIS

Two LLDPE resins were used in this work to determine the critical conditions for the occurrence of wall slip and melt fracture in capillary extrusion. It was found that the polymer–metal interface fails at a critical value of the wall shear stress of about 0.1 MPa and, as a result, slip occurs. At values of wall shear stress of about 0.18 MPa the extrudate surface appears to be matte, while small amplitude periodic distortions (sharkskin) appear on the surface of extrudates at wall shear stresses above 0.25 MPa. Using a special slit die, the polymer–wall interface was coated with Teflon™ in order to examine the effect of this coating on the processability of polyethylenes. It was found that use of Teflon™ promotes slip, thus reducing the power requirement in extrusion and, most importantly, eliminates sharkskin at high extrusion rates. © 1995 John Wiley & Sons, Inc.

INTRODUCTION

It is known that during polymer melt extrusion irregularities/defects appear on the surface of extrudates whenever the wall shear stress exceeds a critical value. This phenomenon, known in general as melt fracture, is been investigated for the past 45 years but it remains one of the most interesting and challenging problems in polymer processing from both the academic and industrial points of view.[1-4]

The appearance of surface defects is a limiting factor for production rates in many industrial operations such as blown film extrusion of polyethylene. Thus, research programs in industry are focused on modifying the molecular architecture of polyethylenes in order to produce resins with good processing characteristics, or resins more resistant to melt fracture. The relationship between molecular architecture and melt fracture is not well understood, and new resins are developed rather on a trial and error basis.

It has also been observed that the matte appearance of the extrudate is accompanied by wall slip and failure of adhesion at the polymer–metal interface in the die land.[3,4] Thus, when the wall shear stress exceeds a critical value, the no-slip boundary condition ceases to be a valid assumption. From the academic point of view, the importance of studying wall slip velocity is twofold. First, it is necessary to have a slip velocity expression to use in the simulation of polymer processes, and second, to understand and explain the origin of extrudate distortion. The relationship between wall slip and extrudate distortion is not well understood.[5-8]

In general, there is some agreement on the causes of the sharkskin phenomenon. The polymer extrudate fractures at the die exit due to an abrupt change in boundary conditions that lead to high stretching rates exceeding the melt strength.[1,5,6,8-10] Kurtz[9] has also pointed out that prior to the critical stretching, a critical shear stress must be exceeded. In support of this view, a more specific explanation of the polymer fracture has been recently proposed by Tremblay,[7] based on a numerical analysis of the flow at the die exit. His calculations have shown that a large negative pressure (hydrostatic tension) exists at the die exit that cavitates the polymer melt close to the die lip, thus leading to interface failure. Recently, Hatzikiriakos[8] performed some calculations for the steady capillary flow of molten polymers by imposing a slip boundary condition. He found that a large

* To whom correspondence should be addressed.

Journal of Applied Polymer Science, Vol. 55, 595-603 (1995)
 CCC 0021-8995/95/040595-09

extensional rate exists at the capillary exit. Based on his calculations, he explained the effects of a number of parameters on extrudate distortion, including length-to-diameter ratio, pressure, diameter, and presence of low surface energy coatings (Vitons™ and Teflons™) at the polymer–wall interface. The extensional rate is a result of a pressure-dependent slip velocity, with the slip velocity being a decreasing function of pressure. Thus, as the polymer approaches the exit of the die, the slip velocity increases and, as a result, the polymer is being accelerated. This acceleration gives rise to the extensional rate.

In this article we study the rheological behavior of two linear low-density polyethylenes (LLDPEs) to identify the critical conditions for the onset of wall slip and melt fracture in capillary extrusion. The slip velocity is calculated as a function of both the wall shear stress and pressure, and the method to perform such calculations is discussed in detail. The relationship between molecular architecture and wall slip is also examined. Finally, the effects of some new low surface energy coatings (Teflon™) on extrudate distortions are also examined.

EXPERIMENTAL

Two linear low-density polyethylenes (LLDPE) were examined in this work. These are Dowlex™ 2049 and HP-LLDPE of Dow Chemicals. The latter is a more viscous resin, but due to the fact that it has a broader molecular weight distribution, exhibits more shear thinning behavior. Some molecular parameters are listed in Table I. The experiments were run at 200°C. Previously reported data on the wall slip of other LLDPEs[11,13] will be compared with those obtained in the present study. The molecular parameters of these resins are also listed in Table I.

Table I Molecular Characteristics of Resins Used

Resin	Melt Index	M_w	I	ρ (g/cm^3)
Dowlex™ 2049	1.0	119,600	3.82	0.926
HP-LLDPE	0.5	161,000	5.20	0.926
Dowlex™ 2045	1.0	118,000	3.93	—
GRSN/7047	1.0	114,000	3.90	—

I is the polydispersity index defined as $I \equiv M_w/M_n$, where M_n is the number-average molecular weight and M_w is the weight-average molecular weight.

Table II Dimensions of Capillary Dies Used

Diameter	Length-to-Diameter Ratio
0.02″	0, 40, 100
0.03″	0, 10, 20, 40, 70, 100
0.05″	0, 40, 70

The experiments were carried out on an INSTRON model 1123 constant-speed piston-driven capillary rheometer. Circular dies of various diameters, D, and length-to-diameter ratios (L/D) were used in order to determine the Bagley correction and slip velocity (Table II). The Bagley correction is essentially determined by making use of orifice dies. To calculate the slip velocity, at least three dies having a constant L/D ratio and different diameter are needed. In this way, one keeps constant the effect of pressure on the slip velocity. Finally, to calculate the slip velocity as a function of pressure, a series of dies of constant diameter and various L/D ratios are required. More details are discussed below.

Slit dies were also used in order to examine the effect of Teflon™ coating on extrudate distortion. The slits were constructed from two pieces so that the interior surfaces could be exposed. It was, thus, possible to apply the Teflon™ solution to the walls of the slit at 160°C. Consequently, enough time was allowed for the solvent to evaporate. More details are given below.

THE BAGLEY CORRECTION

To determine the pressure drop associated with changes in the velocity distribution in the entrance and exit regions, a technique outlined by Bagley[14] was employed. However, when the effect of pressure on viscosity is significant, the Bagley plot curves up. In such cases a quadratic interpolation is recommended[15] in order to extrapolate to zero L/D ratio. Another technique to determine the Bagley correction is to make use of orifice capillaries dies (L/D = 0). It was found in this study that both methods gave similar results.

Figure 1 is a plot of the Bagley correction for the two LLDPE resins determined by making use of the orifice capillaries dies (three dies in total having different diameters and 90° entrance angle). It can be seen that the Bagley correction determined by using three orifice dies having a different diameter superposes very well for both resins. Also, it can be seen

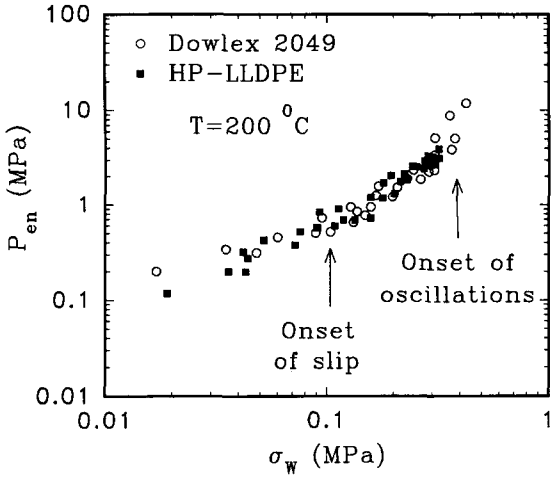

Figure 1 The Bagley correction for Dowlex® 2049 and HP-LLDPE at 200°C.

that the Bagley correction function is the same for both resins due to the similar rheological characteristics of the two resins. The resin HP-LLDPE is more viscous at low values of shear stress, but due to the fact that it has a broader molecular weight, it is more shear thinning resin than Dowlex® 2049.

It can also be observed from Figure 1 that there is a change of slope of the Bagley correction function at about 0.1 MPa, which is the critical shear stress for the onset of slip. Also, there is an apparent discontinuity in the Bagley correction function for wall shear stresses greater than about 0.35 MPa, which is the critical stress for the onset of oscillating melt fracture. Similar observations were reported by Lupton and Regester.[16] However, at this point it is not known if these observations are simply a coincidence. More data are needed to support or disprove these observations.

A METHOD TO DETERMINE THE SLIP VELOCITY

Wall slip phenomena in linear polyethylenes have been studied in the past by many research groups.[3,4,16–18] However, only recently was it observed by Hill et al.[19] that the slip velocity of a linear low-density polyethylene reported by Kalika and Denn[3] was a weak function of the L/D ratio of the capillary for long capillaries (L/D > 33), thus indicating that the slip velocity is a weak function of pressure at high pressures. This was also confirmed for a series of high-density polyethylenes by Hatzikiriakos and Dealy.[15] They reported that the slip velocity was a strong function of the L/D ratio for short dies and a weak function of L/D for long dies.

The viscosity of linear low-density polyethylenes is a function of pressure.[3,20] The traditional Mooney analysis to determine the slip velocity requires that both the viscosity and the slip velocity are not functions of pressure. Thus, this technique cannot be applied to determine the slip velocity as a function of both pressure and wall shear stress. A modified Mooney technique for calculating the slip velocity as a function of both wall shear stress and pressure was recently developed.[15] This technique will also be used here with the addition that the pressure dependency of the viscosity of the melt should be taken into account.

Kalika and Denn,[3] in their slip velocity calculations for a LLDPE, took into account the pressure dependency of viscosity. They have demonstrated their method with data obtained from relatively long capillaries. In such capillaries the slip velocity is only a weak function of pressure. The calculated slip velocity based on the total pressure drop is about equal to the length-averaged slip velocity. However, this is not the case in short capillaries where a slip velocity based on the total pressure drop is not equal to the length-averaged slip velocity.

The two techniques proposed by Kalika and Denn[3] and Hatzikiriakos and Dealy[15] can be combined to develop a method that can be used to calculate the slip velocity as a function of wall shear stress and L/D ratio for polymer melts with a pressure-dependent viscosity. Note that since the slip velocity is a function of pressure, neither the wall shear stress nor the slip velocity are constants along the capillary, as normally assumed in the traditional Mooney analysis. These quantities are functions of the axial distance. In this case, from the pressure drop along the capillary one may only calculate the wall shear stress and the corresponding slip velocity at some axial distance.[15]

If the viscosity of the melt is a function of pressure, it can be represented by the following equation:

$$\eta = K \exp(\beta P)\, \dot{\gamma}^{n-1} \qquad (1)$$

where η is the viscosity, K is the consistency index, n is the power-law index and β is the pressure coefficient of viscosity. The exponential dependence of the viscosity on pressure $\eta \propto \exp(\beta P)$ is usually valid to first order for relatively small values of pressure. Unfortunately, the validity of this relation can only be checked at low and moderate pressures (see below), due to the fact that at higher values of pressure slip occurs and, thus, the effect of pressure

on viscosity cannot be distinguished with certainty from the effect of pressure on slip velocity. Thus, the analysis of our data presented below assumes that Eq. (1) is also valid for high pressures.

To calculate the slip velocity, one may use Eq. (2):

$$\frac{8u_s(z_0)}{D} = \dot{\gamma}_A - \frac{4n}{3n+1}\left(\frac{\sigma_{wp}(z_0)}{K}\right)^{1/n} \qquad (2)$$

where $\dot{\gamma}_A$ is the apparent shear rate defined as $32Q/\pi D^3$, where Q is the volumetric flow rate and D is the diameter of the capillary, u_s is the slip velocity, and σ_{wp} is the pressure-corrected wall shear stress defined below. The value z_0 is some axial distance in the capillary, where the wall shear stress is equal to $(P_d - P_{en})/(4L/D)$, P_d being the driving pressure (plunger force over the reservoir cross-sectional area), and P_{en} being the entrance pressure loss (Bagley correction). The pressure at this point can be approximated as to be equal to $(P - P_{en})/2$. More details regarding the modified Mooney technique can be found elsewhere[15].

The pressure-corrected wall shear stress can be calculated from the following equations:

$$\sigma_w = K \exp[\beta P(z_0)]\left[\frac{3n+1}{4n}\dot{\gamma}_A\right]^n \qquad (3)$$

$$\sigma_{wp} = \frac{\sigma_w}{\exp[\beta P(z_0)]} \qquad (4)$$

where the pressure coefficient of viscosity was found to be about 4×10^{-9} Pa^{-1} for both resins studied in this work. Equation (2) is valid only if the rheology of the melt in the slip region can be described by Eq. (3). Otherwise, one has to use the Modified Mooney technique,[15] that is:

$$\dot{\gamma}_A = \dot{\gamma}_{A,s} + \frac{8u_s(z_0)}{D} \qquad (5)$$

where $\dot{\gamma}_{A,s}$ is the apparent shear rate corrected for slip which is a function of the wall shear stress at the axial position z_0. Use of Eq. (5) requires the determination of the apparent flow curve for at least three capillaries having different diameter and constant length-to-diameter ratio. The latter is necessary in order to keep constant the effect of pressure on both viscosity and slip velocity.

THE SLIP VELOCITY

The slip velocity calculations will be demonstrated for the first resin in Table I (Dowlex™ 2049), whereas only the final results will be presented for the other resins. Figure 2 shows the apparent flow curve of the LLDPE (Dowlex™ 2049) for three capillaries of the same length-to-diameter ratio (L/D = 40) and different diameters. Note that a semi-log plot is used to show clearly the critical shear stress for the onset of slip. As may be seen from Figure 2, the critical shear stress, σ_C, can be determined from the point at which the three apparent flow curves diverge; that is, about 0.10 MPa. This value is consistent with other values reported in the literature for LLDPEs of comparable molecular weight and distribution.[4,21] A value of 0.1 MPa was also found for resin HP-LLDPE. These critical values as well as other constants for the resins are listed in Table III. The continuous curve represents Eq. (3) with pressure corresponding to a capillary having a length-to-diameter ratio of 40.

Once the critical shear stress has been determined, one may use the data in the no-slip region ($\sigma_w < 0.1$ MPa) to obtain the pressure-dependency coefficient of viscosity. Figure 3 plots the pressure-corrected flow curves for Dowlex™ 2049 and compares those with data obtained from the sliding plate rheometer (ambient pressure). One may see that the degree of superposition of data obtained from two different rheometers is reasonable. The contin-

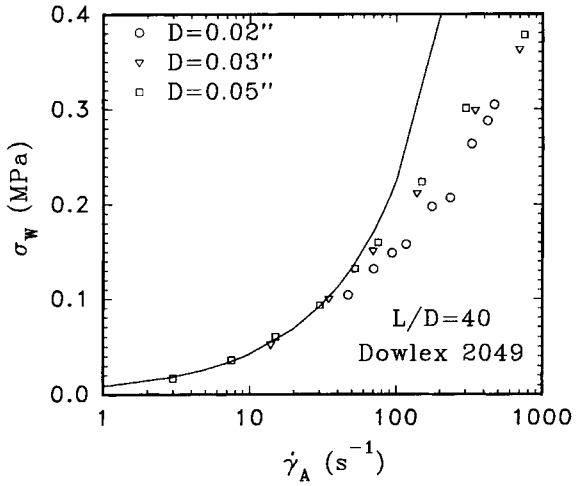

Figure 2 Apparent flow curves of Dowlex™ 2049 at 200°C determined with capillaries having a constant length-to-diameter ratio (L/D = 40) and various diameters.

Table III Critical Stresses and Rheological Parameters of Resins in Table I.

Resin	T (°C)	K (MPa·s^n)	n	β (MPa^{-1})	σ_c (MPa)
Dowlex™ 2049	200	0.0081	0.674	0.0040	0.10
HP-LLDPE	200	0.0149	0.540	0.0040	0.10
Dowlex™ 2045	215	0.0085	0.618	0.0035	0.10
GRSN/7047	200	0.0108	0.603	—	0.10

The Results for Dowlex™ 2045 were reported in Ref. 13 and those for GRSN/7047 in Ref. 11.

uous line represents Eq. (3) with $P = 0$. Finally, apparent flow curves obtained from dies having the same diameter but different L/D ratios are plotted in Figure 4. Note that these apparent flow curves have not been corrected for the effect of pressure on the polymer viscosity.

Using Eqs. (2), (3), and (4), and the data of Figure 2, the slip velocity can be calculated as a function of the wall shear stress for each die separately. If Eq. (5) is valid in the slip region, then a reasonable superposition of the slip data is expected. Equation 5 (modified Mooney technique) was also used to determine the slip velocity. Figure 5 is a Mooney plot. The slip velocity can be inferred from the slopes of straight lines fitted to the data. It can be seen that the data do not fall on a straight line. This may be due to the viscous heating effect that is more significant for capillaries having a larger diameter provided that the length-to-diameter ratio is kept constant.[21] The effects of viscous heating were also discussed by Shidara and Denn,[22] who have pointed out that a numerical solution of the full field incorporating pressure and temperature effects is needed. In our case, the effect of viscous heating appears to be small, and a straight line can still be fitted to data.

Figure 6 plots the slip velocity data calculated for each capillary diameter by making use of Eq. (2) and the slip velocity data by using the modified Mooney technique [Eq. (5)]. The good superposition of the slip velocity data indicates that Eq. (3) is valid, and the rheology of the polymer can be described by using a power-law expression with a pressure-dependent viscosity. The same was also found for the other resin HP-LLDPE. The constants for the power-law expression for all resins are listed in Table III.

Using Eqs. (2), (3), and (4), and the data of Figure 4, the slip velocity is calculated as a function of both wall shear stress and pressure. It is plotted in Figure 7. It may be seen that the slip velocity increases with wall shear stress, but decreases with

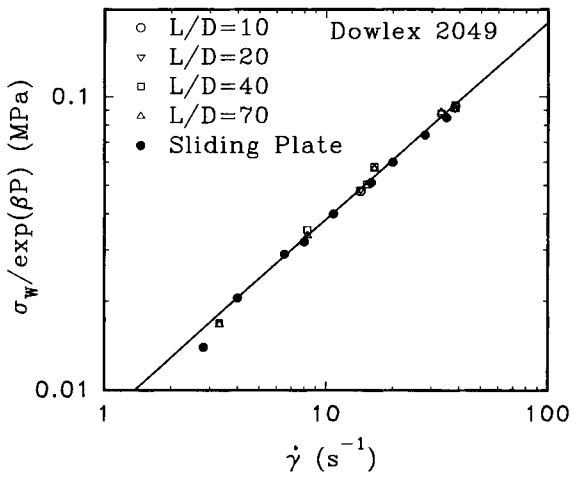

Figure 3 Pressure-corrected flow curves of Dowlex™ 2049 at 200°C in the no-slip region.

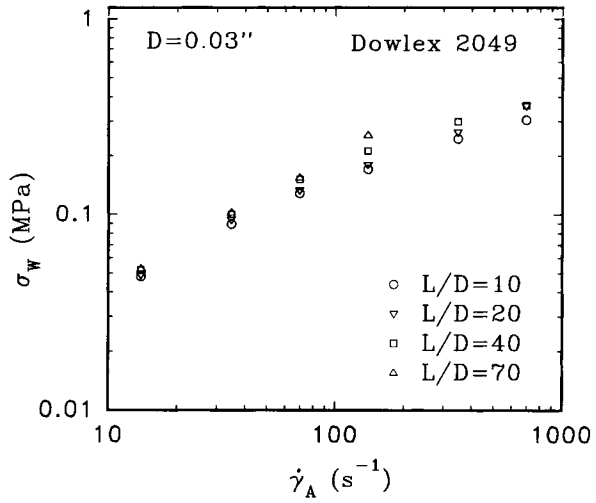

Figure 4 Apparent flow curves of Dowlex™ 2049 at 200°C determined with capillaries having a constant diameter and various length-to-diameter ratios.

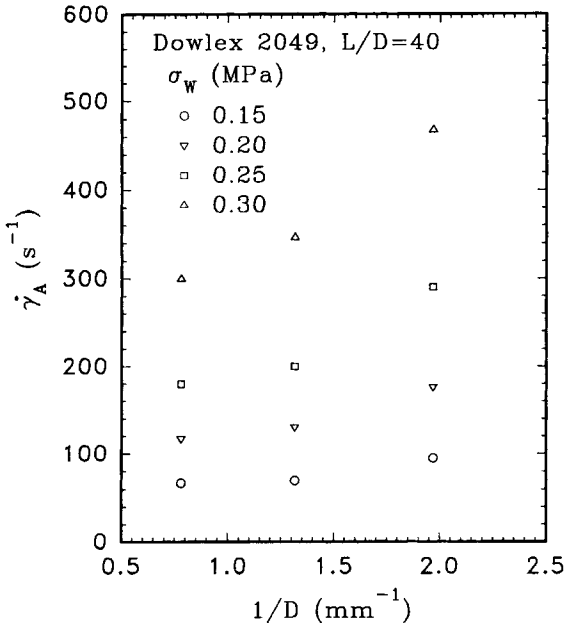

Figure 5 Slip velocity calculations for Dowlex™ 2049 at 200°C using a modified Mooney technique.

increase of the L/D ratio and, thus, pressure. These observations are in agreement with experimental findings reported previously.[13,15,19] Finally, it can be observed from Figure 7 that each curve for a given L/D ratio can be approximately represented by a power law expression ($u_s \propto \sigma_w^m$).

A slip velocity model was recently developed by Hatzikiriakos and Dealy,[15] which incorporates the effects of wall shear stress, wall normal stress (or pressure), temperature, and molecular characteristics of polymers. This can be written as follows:

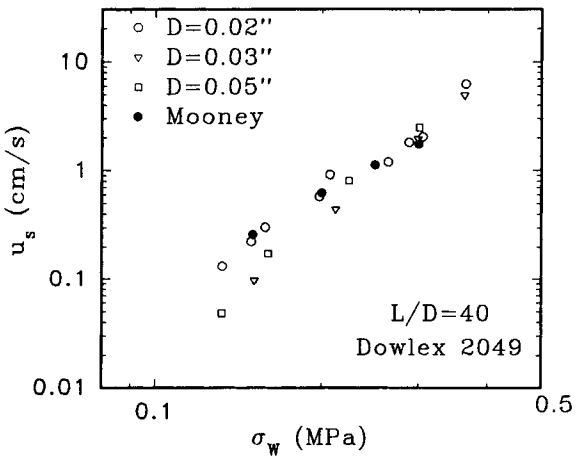

Figure 6 The slip velocity of Dowlex™ 2049 as a function of the wall shear stress at 200°C using capillaries having a length-to-diameter ratio of 40.

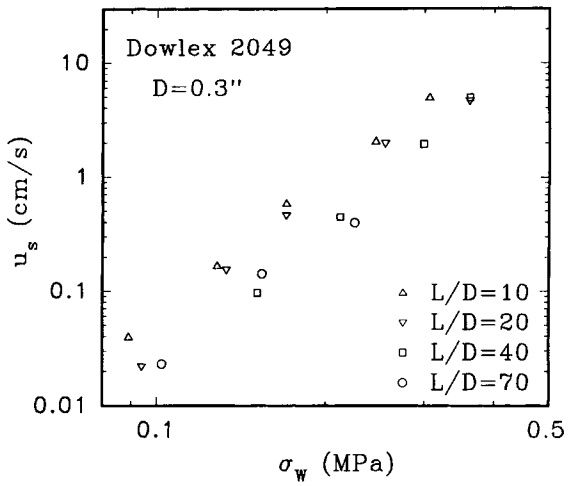

Figure 7 The slip velocity of Dowlex™ 2049 as a function of the wall shear stress and L/D ratio at 200°C. Note that the slip velocity decreases with L/D ratio.

$$u_s = \xi_0 f(T)\left(1 - c_2 \tanh \frac{E + c_3 P/\sigma_w}{RT}\right)\left(\frac{\sigma_w}{\sigma_c I^{1/4}}\right)^m \tag{6}$$

where ξ_0, c_2, c_3, and E are constants, $f(T)$ is a function that incorporates most of the temperature dependence of the slip velocity, and I is the polydispersity of the material. Using Eq. (6), the slip velocities of Figure 5 can be corrected for the effect of pressure in order to refer all of them to ambient pressure. This can be done by using Eq. (7)

$$u_{s,P=0} = u_s(P)\frac{1 - c_2 \tanh[(E/RT)}{1 - c_2 \tanh(E + c_3 P/\sigma_w)/RT]} \tag{7}$$

where $u_{s,P=0}$ is the slip velocity at ambient pressure and $u_s(P)$ is the slip velocity at pressure P, which is being corrected to refer to ambient pressure. Figure 8 shows the pressure-corrected slip velocities, $u_{s,P=0}$ of Figure 7 and those for the other three resins. Note that all these slip velocities now refer to ambient pressure. To take into account molecular architecture effects, the data are plotted vs. the normalized wall shear stress, $\sigma_w/\sigma_c I^{1/4}$. The values of the parameters used were the ones calculated by Hatzikiriakos and Dealy[15] for a series of HDPEs (c_2 = 0.987, c_3 = 31, and E = 1367 cal/g-mol). In general, the data superposes to a reasonable degree. A better superposition could have been obtained by reevaluating the constant c_2, c_3, and E. The data for Dowlex™ 2045 was obtained from Ref. 13 and

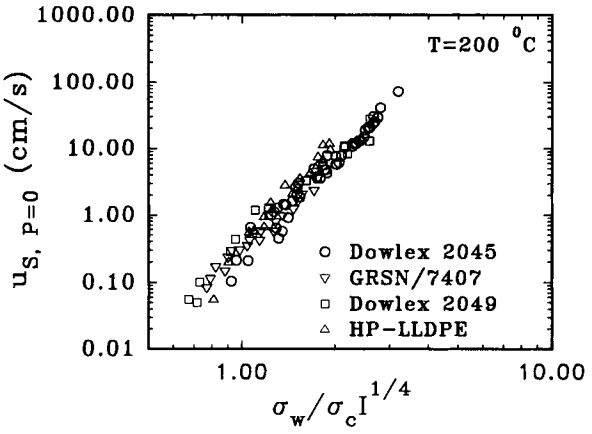

Figure 8 The pressure-corrected slip velocity, $u_{s,P=0}$ of various LLDPEs as a function of the normalized wall shear stress, $\sigma_w/\sigma_c I^{1/4}$, at 200°C. The slip velocity data now refers to ambient pressure.

those for GRSN/7407 from Ref. 11. Note that the data for GRSN/7407 were obtained by using a sliding plate rheometer and, thus, the use of Eq. (7) was not necessary.

The molecular weight and distribution is the same for three of the resins and, thus, there is no question why these three sets of data agree. The resin HP-LLDPE has a considerably higher molecular weight than the others and, thus, one expects its slip velocity to be higher due to the fact that the shear stress for the onset of slip decreases with increase of the molecular weight.[15] However, its molecular weight distribution is broader, which decreases the slip velocity according to Eq. (6). Thus, the combined effect of molecular weight and its distribution superposed the data. Finally, it is noted that for a given polydispersity the slip velocity increases with molecular weight, while for a given molecular weight the slip velocity decreases with increase of polydispersity.[15]

MELT FRACTURE

Clean Surface

Although the onset of slip occurs at a critical shear stress of about 0.1 MPa, the extrudates appear to be matte at much higher values of shear stresses (0.18 MPa). Small amplitude periodic distortions appear on the extrudate surface at even higher values of shear stress, essentially above 0.25 MPa for all resins. Oscillating melt fracture was also observed for both resins studied here at a critical shear stress in the range of 0.35–0.4 MPa, this depending on the L/D ratio and the capillary diameter. The oscillating flow regime of polyethylenes was previously analyzed[23] to a great extent and, thus, it will no longer be discussed here.

In general, it was found that at a given apparent shear rate the extrudate distortion increases in severity with length-to-diameter ratio. This is due to the fact that for a given apparent shear rate, higher shear stresses are obtained in longer dies due to the pressure dependency of viscosity. Numerous photographs have been reported previously[2,3,10,23] for all types of melt fracture in polyethylene extrusion with clean surfaces and, therefore, it was decided not to present any here.

Teflon℠-Coated Surface

To study the effect of Teflon℠ coatings on melt fracture, three special slit dies were used. These were constructed from two pieces so that the interior surface could be exposed. It was, thus, possible to apply the coating to the walls.[24] Dimensions and design characteristics of the slit dies used can be found elsewhere.[24] The coating used to modify the polymer–wall interface was Teflon℠, which was provided by DuPont, Wilmington DE, in the form of solution. The solution was applied to the walls and then the solvent was allowed to evaporate at about 160°C.

Photographs of the extrudates were taken to show the effects of the Teflon℠ coating on the extrudate appearance. It was found that the presence of this coating suppresses completely extrudate distortion at all shear rates attained in this study (up to about 1,500 s^{-1}). It is noted that with clean plates sharkskin melt fracture appears at an apparent shear rate of about 250^{-1}. Figure 9 shows extrudates (Dowlex℠ 2049) at two different apparent shear rates for clean and Teflon℠-coated surfaces. It can clearly be seen that the periodic extrudate distortions are completely suppressed. It is noted that there is also a decrease in the extrudate swell with Teflon℠-coated surface that is due to the presence of wall slip.

The suppression of extrudate distortion is accompanied by a reduction in the applied load with Teflon℠-coated surfaces. Extruding an amount of resin equivalent to the volume of the rheometer reservoir, the load is decreased by about 20%, as compared to that obtained during extrusion using the slit die with clean surfaces. A further load reduction is obtained if the rheometer is reloaded and extrusion continues. This indicates that the Teflon℠ coating smooths out with time and provides a better surface for polymer slippage. Thus, it is expected that Tef-

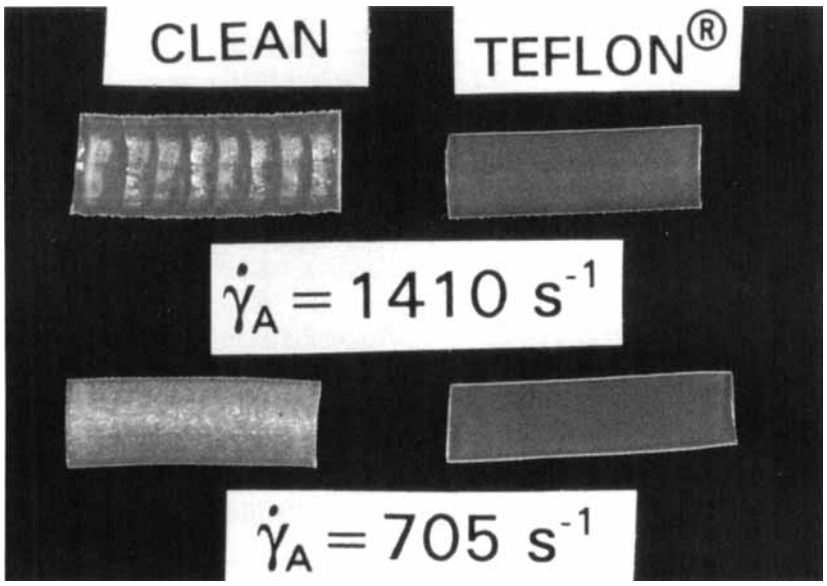

Figure 9 The effect of Teflon™ on the extrudate distortion of Dowlex™ 2049 at two apparent shear rates. The widths of the samples are in the range 0.6–0.8 cm.

lon™ as a coating or as an additive to polymer resins will be a very efficient processing aid to suppress extrudate distortion and to reduce power consumption.

CONCLUSIONS

In this work, the slip velocity of two new polyethylene resins was calculated as a function of both wall shear stress and pressure. It was found that the slip velocity increases with shear stress and decreases with pressure. The calculated slip velocities were compared with others reported previously in the literature for LLDPEs and found to be consistent with the molecular characteristics of resins. A model previously proposed in the literature for the slip velocity of high density polyethylenes was found to be capable of describing the slip velocity of linear low density polyethylenes as well. Thus, once slip data were corrected for the effects of pressure by using this model, they superposed very well.

A new Teflon™ coating was used to coat the side walls of a special slit die in order to study its effect on wall slip and extrudate appearance. First, it was found that the presence of this coating at the interface increases slip, thus reducing power requirement for extrusion. Second, but most importantly, it was found to suppress completely extrudate distortion up to apparent shear rates of 1,500 s^{-1} (maximum attainable shear rate with the slit dies used) while extrudate distortion first appears with clean surfaces at a rate of 250 s^{-1}.

Financial assistance from the Natural Sciences and Engineering Research Council of Canada is greatly appreciated. Additional financial support from DuPont & de Nemours, Wilmington, DE, is also appreciated.

REFERENCES

1. E. R. Howells and J. J. Benbow, *Trans. Plast. Inst.*, **30,** 240–253 (1962).
2. N. Bergem, in *Proceedings of the 7th Intnational Congress on Rheology,* Swedish Society of Rheology, Gothenberg, 1976, p. 50.
3. D. S. Kalika and M. M. Denn, *J. Rheol.*, **31,** 815 (1987).
4. A. V. Ramamurthy, *J. Rheol.*, **30,** 337 (1986).
5. N. F. Cogswell, *J. Non-Newt. Fluid Mech.*, **4,** 23 (1978).
6. N. F. Cogswell, *J. Non-Newt. Fluid Mech.*, **2,** 37–47 (1977).
7. B. Tremblay, *J. Rheol.*, **35,** 985–998 (1991).
8. S. G. Hatziriakos, *Polym. Eng. Sci.* (to appear).
9. S. J. Kurtz, in *Advances in Rheology,* vol. 3, B. Mena, A. Garcia-Rejon, and C. Rangel-Nafaille, Eds., UNAM Press, Mexico, 1984, pp. 399–407.
10. R. H. Mounihan, D. G. Baird, and R. Ramanathan, *J. Non-Newt. Fluid Mech.*, **36,** 255 (1990).
11. S. G. Hatzikiriakos, C. W. Stewart, and J. M. Dealy, *Int. Polym. Proc.*, **VIII,** 31 (1993).

12. S. G. Hatzikiriakos and J. M. Dealy, *Int. Polym. Proc.*, **VIII,** 36 (1993).
13. C. Tzoganakis, B. C. Price, and S. G. Hatzikiriakos, *J. Rheol.*, **37,** 355–366 (1993).
14. E. G. Bagley, *J. Appl. Phys.*, **28,** 624 (1957).
15. S. G. Hatzikiriakos and J. M. Dealy, *J. Rheol.*, **36,** 703 (1992).
16. J. M. Lupton and J. W. Regester, *Polym. Eng. Sci.*, **5,** 235 (1965).
17. L. L. Blyler and A. C. Hart, *Polym. Eng. Sci.*, **10,** 193 (1970).
18. T. F. Ballenger, I. J. Chen, J. W. Crowder, G. E. Hagler, D. C. Bogue, and J. L. White, *Trans. Soc. Rheol.*, **15,** 195 (1971).
19. D. A. Hill, T. Hasegawa, and M. M. Denn, *J. Rheol.*, **34,** 891 (1990).
20. I. J. Duvdevani and I. Klein, *SPE J.*, **23,** 41 (Dec. 1967).
21. R. M. Ybarra and R. E. Eckert, *AIChE J.*, **26,** 751 (1980).
22. H. Shidara and M. M. Denn, *J. Non-Newt. Fluid Mech.*, **48,** 101 (1993).
23. S. G. Hatzikiriakos and J. M. Dealy, *J. Rheol.*, **36,** 845 (1993).
24. S. G. Hatzikiriakos and J. M. Dealy, *Int. Polym. Proc.*, **VIII,** 36 (1993).

Received May 16, 1994
Accepted May 22, 1994